Rail steel flaw inspection based on laser ultrasonic method

Nan Gangyang, Wang Qiwu, Zhang Zhenzhen, Guo Rui, Song Jiangfeng, Sun Jihua

(Nondestructive Testing Lab, Laser Institute of Shandong Academy of Sciences, Jinan 250103, China)

Abstract: To meet reliability of rail steel flaw inspection and signal acquisition, a nondestructive testing (NDT) system based on laser ultrasonic technique (LUT) was established. The system was mainly composed of high energy pulse laser, electromagnetic ultrasonic transducer (EMAT), embedded data acquisition system and P60 rail specimens with artificial cracks. Based on analysis of Rayleigh wave detection principle, this paper focuses on impedance matching method of EMAT probe coil. Besides, working flow path and signal processing of embedded signal acquisition system were introduced. Moreover, system based LUT was used to locate the rail steel surface crack with depth no less than 0.5 mm. Finally, relationship between EMAT probe lift-off distance and signal amplitude was given.

Key words: laser ultrasonic; rail steel flaw inspection; EMAT

CLC number: TB552 **Document code:** A **DOI:** 10.3788/IRLA201746.0106006

基于激光超声方法的钢轨缺陷检测

南钢洋,王启武,张振振,郭 锐,宋江峰,孙继华

(山东省科学院激光研究所无损检测平台, 山东 济南 250103)

摘 要: 针对钢轨探伤可靠性试验及缺陷信号采集处理要求, 建立了一套基于激光超声技术的无损检测系统。该系统主要包括高能量脉冲激光器、电磁超声换能器、嵌入式信号采集处理系统以及带有人工缺陷裂缝的 P60 钢轨试件。在分析利用瑞利波探伤机理的基础上,重点研究了激励线圈阻抗匹配方法,介绍了嵌入式信号采集处理系统工作原理及其信号处理过程。最后利用搭建的激光超声检测系统,实现钢轨表面深度不少于 0.5mm 缺陷的定位,并给出了接收信号幅度与提离距离以及缺陷尺寸的关系。

关键词: 激光超声; 钢轨探伤; 电磁超声换能器

收稿日期:2016-05-21; **修订日期**:2016-06-23

基金项目:山东省科学院青年基金(2013QN008);山东省自然科学基金(ZR2016FB26)

作者简介:南钢洋(1984-),男,助理研究员,博士,主要从事超声检测和数据获取方面的研究。Email:slightcloud2004@aliyun.com

0 Introduction

With development of high-speed railway, rail steel inspection based on NDT technique plays an important role in normal safety operation. Many rail flaws such as cracks, holes or other defects may occur unexpectedly and impact potential safety hazards to human life [1]. One of the fatal flaws is surface crack, so related inspection and research are indispensable[2-3].

To inspect and locate these surface cracks, traditional inspection methods have been used, such as piezoelectric ultrasonic, magnetic particle and eddy current. Nevertheless, these methods need couplant to match the acoustic impedance between transducer and rail steel [2-4]. Moreover, when couplant is mixed with lubricant on railhead, the echo intensity descends, which increases error rate of detections[5-6].

In recent years, laser ultrasonic technique (LUT) has been developed rapidly; it can overcome those disadvantages of traditional inspection [7]. Now system based LUT can help manufactures to examine equipments quality, also it can work properly without couplant or highly smooth surface. Furthermore, it is capable to work under harsh conditions, such as high temperature, high pressure and poisonous air[8].

When pulse laser beams irradiate on rail steel surface, several types of ultrasonic waves are excited, including longitudinal waves, shear waves and Rayleigh waves. These ultrasonic waves can be received by EMAT method. However, the signal-noise ratio (SNR) for EMAT signals was not good, and flaw signals were not clear in ultrasonic frequency domain which is about 50 kHz-4 MHz.

So the aim of this work is to realize a better SNR for flaw signals with proper design of EMAT coils. To achieve the aim, EMAT probe coil model and method for coils impendence matching would be researched. Also, Rail steel flaw inspection system is established with Q-switched Nd: YAG pulse laser, embedded signal acquisition system DAQ600 and P60 rail steel specimens. Through receiving ultrasonic waves by EMAT probe, the ultrasonic signals were sampled by DAQ600, and cracks can be located in real time on local computer.

1 Laser ultrasonic wave inspection and EMAT probe coil model

1.1 Laser ultrasonic wave inspection

Generally, pulse laser can excite point beams and line beams using round lens and cylindrical lens respectively. According to ultrasonic wave generation theory, inspection can be divided into thermo elastic mode and ablation mode. When irradiated by laser beams, rail steel specimen surface is heated based on thermo elastic effect, and several types of ultrasonic waves are generated simultaneously with different frequency bands and propagation speeds, including shear waves, longitudinal waves, and Rayleigh waves.

Figure 1 indicates Rayleigh wave propagation direction. Via cylindrical lens, laser pulses are focused line beams on the rail steel surface. At the same time, Rayleigh waves are generated and their energy is mainly concentrated in normal direction of the focus line beam.

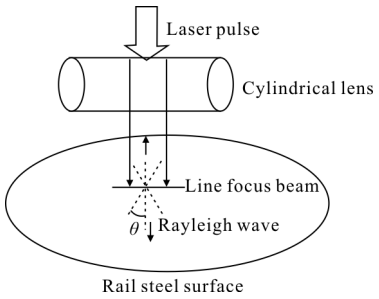

Fig.1 Rayleigh wave propagation direction

This directivity characteristic is available to inspect the rail steel surface flaws. Formula (1)[9] can be utilized when calculating wave propagation direction.

$$R_\theta=\frac{\sin(\pi lv/CR)\sin\theta)}{(\pi lv/CR)\sin\theta)} \tag{1}$$

Where l is laser pulse length; v represents ultrasonic wave frequency; θ is angle between Rayleigh wave

propagation direction and normal line of the focus beams, and *CR* represents Rayleigh wave speed. When Rayleigh waves propagate in the material with Poisson ratio range at about 0−0.5, *CR* is given by[10]

$$CR \approx \frac{0.87+1.12\sigma}{1+\sigma} ct \tag{2}$$

Where σ means Poisson ratio; its value is about 0.29 for P60 rail steel; *ct* is shear wave speed in normal atmospheric temperature.

1.2 EMAT probe coil model

Figure 2 indicates model of inspection system based on LUT for P60 rail steel specimen. The EMAT probe mainly consists of coils, NdFeB magnet, carbonyl iron powder sheet, SiC ceramic plate, pre−amplifier circuit and an oxidation−resisting shell. Once pulse laser beams irradiate on rail steel surface, Rayleigh waves are generated and propagate forward in the central axis direction, and they can be reflected and converted into shear waves when transmitting through area with different acoustic impedance, such as cracks or interior holes.

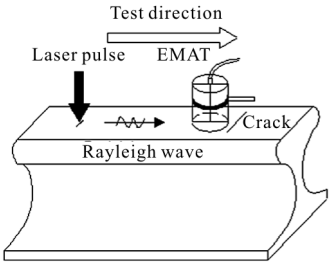

Fig.2 Rail steel surface flaw detecting model

On the other hand, only when EMAT probe is vertical above the cracks, the wave signal amplitude reaches maximum. Through locating the maximum value, cracks can be inspected.

The EMAT probe coil was designed as four layers Printed Circuit Board (PCB) with butterfly structure as illustrated in Fig.3(a). When ultrasonic waves propagate below EMAT probe, the probe coils cut magnetic induction lines in perpendicular magnetic field, and then coils generate differential signals contained the rail steel crack information.

After amplified and filtered by analog circuits, the ultrasonic wave signals are sampled by data acquisition system. At last, the rail steel crack information can be extracted via data processing and analysis. By this design, the common mode noise can be decreased, and the Signal−to−Noise Ratio (SNR) index would be improved.

Figure 3 shows EMAT probe coil structure and its equivalent circuit. Adopting this coil, ultrasonic waves can be coupled effectively and converted to differential current signals, which indicate position and size of the cracks. For coil design, many parameters can affect EMAT probe coil impedance and its response frequency characteristic, such as material type and coil structure.

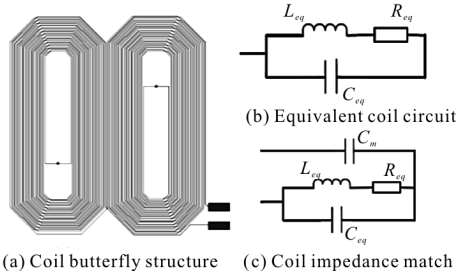

Fig.3 EMAT probe coil butterfly structure

Figure 3(b) indicates the equivalent circuit of EMAT probe coil. To maximize amplitude of ultrasonic wave signal, impedance matching capacitor C_m is used to parallel with the probe coils as Fig.3(c) shows. The admittance for this parallel circuit is given by:

$$Y_{eq}=\frac{R_{eq}}{R_{eq}^2+(\omega_0 L_{eq})^2}+j(\omega_0(C_m+C_{eq})-\frac{\omega_0 L_{eq}}{R_{eq}^2+(\omega_0 L_{eq})^2}) \tag{3}$$

Where ω_0 is center an gular frequency of laser pulse signal; Y_{eq} is the matched circuit admittance; L_{eq} is equivalent inductance; R_{eq} is equivalent resistance and C_{eq} is equivalent capacitance.

When the capacitance matched circuit is in parallel resonance, Y_{eq} reaches minimum, and its imaginary part equals to zero.

$$\omega_0(C_m+C_{eq})-\frac{\omega_0 L_{eq}}{R_{eq}^2+(\omega_0 L_{eq})^2}=0 \tag{4}$$

So C_m value is given by

$$C_m=\frac{L_{eq}}{R_{eq}^2+(\omega_0 L_{eq})^2}-C_{eq} \tag{5}$$

After impedance matching, the ultrasonic wave signal bandwidth becomes narrow and signal amplitude can achieve maximum. This is conducive to improve SNR of the EMAT signal.

2 Introduction for DAQ600 system

Based on "ARM +FPGA +ADC" architecture, DAQ600 framework is depicted in Fig.4. With 16 bit pipeline ADC, DAQ600 system supports 125MSPS sampling. Also the system supports state monitoring, digital I/O port expansion and 100 Mbps Ethernet. Furthermore, DAQ600 has high power efficiency and excellent electromagnetic compatability (EMC) performance.

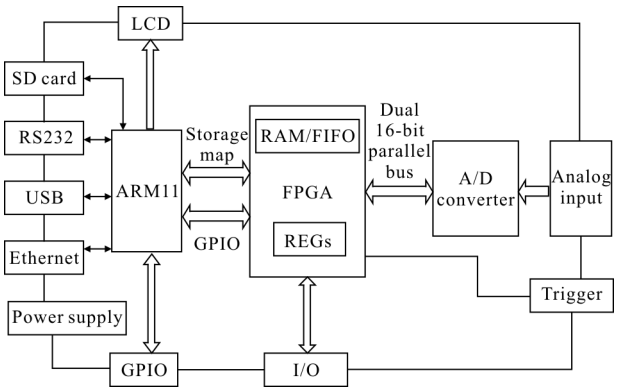

Fig.4 DAQ600 system framework

To synchronize with laser excitation, a photodiode module is used to generate trigger signal. After receiving a rising edge of the trigger, FPGA starts finite state machine and controls ADC to convert the received signals into 16 bit data, and then these data are filtered and stored in on-chip dual-port RAM of FPGA. Then the data are fetched by ARM through a parallel bus via a SROM controller with transmission speed of 133 Mb/s. After uploaded via Ethernet, the ultrasonic data can be processed and analyzed effectively by computer on line.

3 Experiment setup

Figure 5 illustrates the overall system of a rail steel experiment based LUT method. It mainly includes Q-switched Nd:YAG pulse laser (1 064 nm, 45 mJ, 10 ns, 20 Hz), optical cylindrical lens, trigger module, P60 rail steel specimen, EMAT probe and computer as well as DAQ600 system. To measure accurately and conveniently, some cracks were carved artificially on rail steel specimen surface, while EMAT probe liftoff distance is 3 mm relative to the specimen surface.

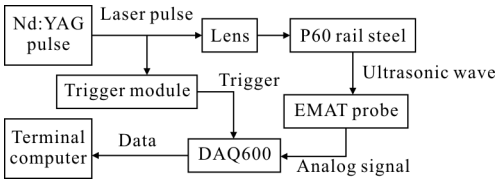

Fig.5 Overall architecture of experiment setup

When laser beams irradiate on rail steel specimen surface via cylindrical lens, Rayleigh waves are generated and spread along specimen's surface. When met with cracks, Rayleigh waves are reflected and converted into shear waves, which would be coupled into current signals by EMAT probe coils, according to Faraday electromagnetic induction law. After adjusted by preamplifier circuit, the coupled current signals are converted to voltage signals.

However, the received waves are mixed with spurious signal sources, such as echo wave signals, random ambient noise, power supply noise and thermal noise. So a π type analog filter and digital band pass filter are used to decrease these noises. With good repeatability, averaging algorithm is taken to improve SNR for the received waves.

4 Results and analysis

For comparison, Figure 6 (a) shows ultrasonic wave with four times average; Figure 6 (b) is wave without any averaging algorithm. In these two figures, x axis indicates time, the scale is 10 μs; y axis indicates ultrasonic signal amplitude; the scale is 50 mV. By comparison, the difference for SNR between these two figures is clear; and Fig.6 (a) has a better SNR than Fig.6 (b). Also, the former has more accuracy maximum.

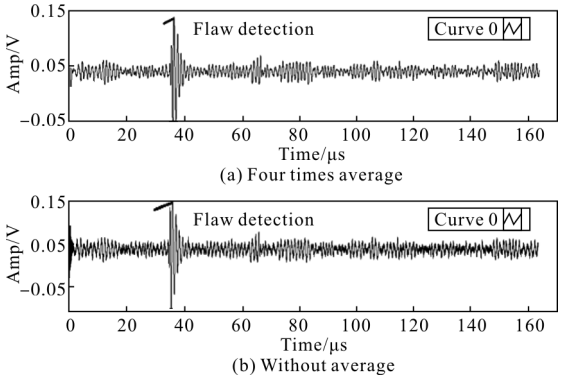

Fig.6 Ultrasonic wave acquisition and displaying

While EMAT probe is vertical above cracks or holes, the received signal amplitude could reach maximum, so the time point in x axis for signal maximum appearance can represent the crack position information. Through calculating time gap Δt between irradiating point and EMAT probe, the crack positions can be measured automatically.

To acquire the ultrasonic signal maximum value, data acquisition software based LabVIEW software has been developed. After starting a maximum searching algorithm, the peak point can be found at 36.16 μs point, and Δt is 36.16 μs. Figure 7 (a) shows the inspection system. The Rayleigh wave path s can be obtained with Formula (6).

$$s=CR\Delta t \tag{6}$$

Where CR is Rayleigh wave speed, which is about 2 890 m/s in P60 rail. According to Formula (6), s=1 04.5 mm, and this is in accordance with verification result as Fig.7(b).

(a) Ultrasonic signals display in real-time

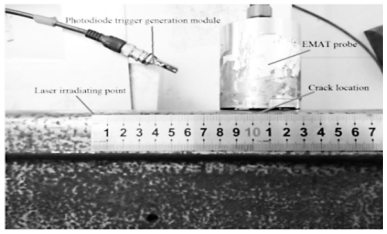

(b) Crack is located

Fig.7 Rail steel flaw detection with DAQ600

Also spectrum of the ultrasonic signal can be analyzed by FFT algorithm; it is depicted in Fig.8. From the spectrum, the major energy of ultrasonic wave signal is concentrated in the frequency band of 0.65−0.85 MHz. Based on this characteristic, digital band pass filter is used to filter noise which is outside the ultrasonic frequency range, and SNR for the ultrasonic signal will be improved.

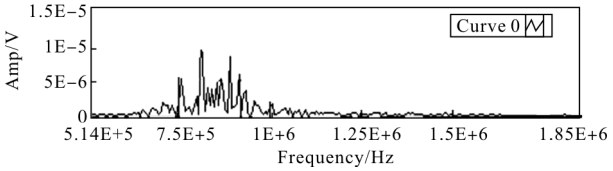

Fig.8 Ultrasonic wave signal spectrum

4.1 Influence of crack size

When artificial surface crack depth becomes larger, amplitude of the received ultrasonic waves increases. That is because the reflected waves are enhanced when Rayleigh waves meet artificial surface cracks, and then reflected waves are converted to shear waves, which are received by EMAT probe. From Tab.1, rail steel #1 with defect size 60 mm×0.2 mm×0.5 mm can generate 0.15 V ultrasonic signal amplitude, while rail steel #3 with defect size 60 mm×0.2 mm×1.5 mm can generate 0.28 V ultrasonic signal amplitude.

Also, rail steel with 0.4 mm surface crack depth is tested; however, the signal maximum is not clear. So this rail steel flaw detection system can inspect and locate the surface crack with depth no less than 0.5 mm.

Tab.1 Relationship between EMAT signal amplitude and surface crack size

Specimen	Inspection wave	Defect type	Defect size/mm length×width × depth	EMAT signal amplitude/V
Rail steel #1	Rayleigh wave	Surface crack	60×0.2×0.5	0.15
Rail steel #2	Rayleigh wave	Surface crack	60×0.2×1.0	0.22
Rail steel #3	Rayleigh wave	Surface crack	60×0.2×1.5	0.28

4.2 Influence of lift-off distance

Figure 9 shows normalized amplitude of the received ultrasonic wave when the EMAT probe is lifted up from the rail steel specimens. It shows that the ultrasonic wave amplitude deceases as the distance between EMAT probe and rail steel specimen increases. And their relationship is according to an exponential function. That is because the magnetic field inside the EMAT probe attenuates fast to make coupling efficiency descend when the lift-off distance increases.

When the lift-off is above 3 mm, the signal amplitude attenuates largely. After a series of test, the best value of lift-off is about 1-3 mm.

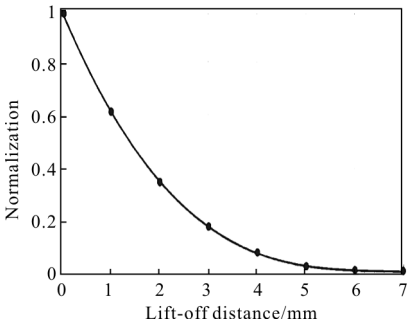

Fig.9 Ultrasonic wave amplitude against EMAT probe lift-off distance

5 Conclusion

This experiment uses Rayleigh wave as the major inspection wave for rail steel surface flaw. Through impendence matching, EMAT coils can receive the Rayleigh wave effectively. According to the experiment result, rail steel flaw can be effectively detected by LUT method and the flaw signals can be acquired by DAQ600 system. After processed and analyzed by LabVIEW software, Rayleigh wave signals containing flaw position can be measured automatically online. This method provides a good solution for rail steel life evaluation.

References:

[1] Zhao Yang, Jia ZhongQing, Guo Rui, et al. The application of laser-EMAT technique used to testing defect in rail[J]. ***Advanced Materials Research***, 2014, 875-877: 574-577.

[2] Clark R. Overview and needs for future developments[J]. ***NDT&E International***, 2004, 37(2): 111-118.

[3] Papaelias M, Roberts C, Davis C. A review on non-destructive evaluation of rails: state-of-the-art and future development[J]. ***Rail Rapid Transit***, 2008, 222(4): 367-384.

[4] Scalea F, Rizzo P, Coccia S, et al. Non-contact ultrasonic inspection of rails and signal processing for automatic defect detection and classification[J]. ***Insight***, 2005, 47(6): 1-8.

[5] Edwards R S, Dixon S, Jian X. Characterisation of defects in the railhead using ultrasonic surface waves [J]. ***NDT&E International***, 2006, 39(6): 468-472.

[6] Fan Y, Dixon S, Edwards R S, et al. Ultrasonic surface wave propagation and interaction with surface defects on rail-track head[J]. ***NDT&E International***, 2007, 40(6): 471-477.

[7] Petcher P A, Potter M D G, Dixon S. A new electromagnetic acoustic transducer (EMAT) design for operation on rail[J]. ***NDT and E International***, 2014, 65: 1-7.

[8] Cheng Jianzheng, Bond Leonard J. Assessment of ultrasonic NDT methods for high speed rail inspection [J]. ***AIP Conference Proceedings***, 2015, 1650(1): 605-614.

[9] Aindow A M, Dewhurst R J, Palmer S B. Laser-generation of directional surface acoustic wave pulses in metals[J]. ***Optics Communications***, 1982, 42(2): 116-120.

[10] Li J W, Chen J M. Nondestructive Testing Handbook[M]. Beijing: China Machine Press, 2001: 202-203.